Modeling Yeast Cell Polarization Induced by Pheromone Gradients

Tau-Mu Yi,[1] Shanqin Chen,[2] Ching-Shan Chou[2] and Qing Nie[2]

Yeast cells respond to spatial gradients of mating pheromones by polarizing and projecting up the gradient toward the source. It is thought that they employ a spatial sensing mechanism in which the cell compares the concentration of pheromone at different points on the cell surface and determines the maximum point, where the projection forms. Here we constructed the first spatial mathematical model of the yeast pheromone response that describes the dynamics of the heterotrimeric and Cdc42p G-protein cycles, which are linked in a cascade. Two key performance objectives of this system are (1) amplification—converting a shallow external gradient of ligand to a steep internal gradient of protein components and (2) tracking—following changes in gradient direction. We used simulations to investigate amplification mechanisms that allow tracking. We identified specific strategies for regulating the spatial dynamics of the protein components (i.e. their changing location in the cell) that would enable the cell to achieve both objectives.

KEY WORDS: G-protein, polarization, gradient-sensing, spatial dynamics, surface diffusion

1. INTRODUCTION

A basic property of cells is asymmetry; from this asymmetry complex structures and behaviors arise.[1] This asymmetry can be directed from internal or external cues. A common type of external cue is a chemical signal; the cell can sense a gradient of the chemical, reorganize its internal components (polarization),

---
[1] Developmental & Cell Biology, Center for Complex Biological Systems, University of California, Irvine, CA 92697, USA; e-mail: tmy@uci.edu
[2] Center for Mathematical and Computational Biology, Center for Complex Biological Systems, Department of Mathematics, University of California, Irvine, CA 92697, USA; e-mail: shanqin@ math.uci.edu; cschou@math.uci.edu; qnie@math.uci.edu

and then move (chemotaxis) or project (chemotropism) toward the source. This process occurs through receptor-mediated signal transduction pathways, and many of the best-studied examples involve a heterotrimeric G-protein system.[2] G-proteins are important signal transduction molecules that are bound to the guanine nucleotide GTP when active and GDP when inactive.

Haploid budding yeast cells (either **a** or α) respond to pheromone gradients in a sensitive and robust fashion that is necessary for efficient mating.[3] During mating, yeast cells undergo polarization and project toward their partner by following a gradient of pheromone. The **a**-cells secrete the pheromone **a**-factor and sense the pheromone α-factor; the α-cells secrete α-factor and sense **a**-factor. Each pheromone binds and activates its cognate pheromone receptor, which in turn catalyzes the activation of the heterotrimeric G-protein, leading to the production of active Gα subunit and free G$\beta\gamma$ dimer.[4]

Directly downstream of the heterotrimeric G-protein in the signaling pathway is the small G-protein Cdc42p, which consists of a single subunit. Free G$\beta\gamma$ binds to Cdc24p, the activator of Cdc42p, and localizes it to the membrane. Active Cdc42p directly mediates a variety of processes necessary for the formation of the mating projection (shmoo), most notably the polarization of the actin cytoskeleton, which facilitates the transport of new proteins to the projection and also serves a structural role. Other functions of Cdc42p include positioning of the polarisome, activation of kinases such as Ste20p and Cla4p, and organization of the septin cytoskeleton.[5]

The complexity of this system can be attributed to the many challenges facing this biological sensor. These performance requirements include sufficient sensitivity so that shallow gradients can be detected, broad dynamic range, tracking moving signal sources, and robustness to internal and external perturbations. Because yeast cells do not move, it is thought that they employ a spatial sensing strategy in which the concentration of pheromone is compared at the front versus back of the cell to determine the direction of the gradient. The high efficiency of yeast mating[6] suggests that this sensing mechanism operates quite proficiently despite the small size of yeast (diameter is 3 to 5 microns). Here we focus on the issues of sensitivity and tracking.

Our model employs a local activation mechanism combining positive feedback and cooperative binding that facilitates the recruitment of proteins to the projection. Simulations reveal the amplification of a shallow external gradient to a steeper internal gradient. This amplification, however, is associated with bistability, which limits the ability of the system to track changes in the gradient direction. We explore how fine-tuning the spatial dynamics of the system (i.e. movement of proteins to different positions in the cell) can enable the cell to achieve both good amplification and tracking.

2. MATHEMATICAL MODEL

The activation and deactivation of a G-protein forms a unidirectional cycle termed the G-protein cycle. Our mathematical model of the yeast pheromone response system centers on the spatial dynamics of the heterotrimeric and Cdc42p G-protein cycles. Previous models of this system have not included spatial information.[7,8] The first four equations of the model represent the dynamics of the heterotrimeric G-protein cycle, and the last four equations represent the dynamics of the Cdc42p G-protein cycle. Many of the parameters of the first cycle have been measured directly or inferred from input-output data.[9] The parameters for the second cycle were estimated from values in the literature.[10]

$$\frac{\partial [R]}{\partial t} = D_m \nabla_m^2 [R] - k_{RL}[L][R] + k_{RLm}[RL] - k_{Rd0}[R] + k_{Rs} \quad (1)$$

$$\frac{\partial [RL]}{\partial t} = D_m \nabla_m^2 [RL] + k_{RL}[L][R] - k_{RLm}[RL] - k_{Rd1}[RL] \quad (2)$$

$$\frac{\partial [G]}{\partial t} = D_m \nabla_m^2 [G] - k_{Ga}[RL][G] + k_{G1}[Gd][Gbg] \quad (3)$$

$$\frac{\partial [Ga]}{\partial t} = D_m \nabla_m^2 [Ga] + k_{Ga}[RL][G] - k_{Gd}[Ga] \quad (4)$$

$$\frac{\partial [C24m]}{\partial t} = D_m \nabla_m^2 [C24m] + k_{24cm0}(Gbg_n^*)[C24c]$$
$$+ k_{24cm1}(B1^*)[C24c] - k_{24mc}[C24m] \quad (5)$$

$$\frac{\partial [C42]}{\partial t} = D_m \nabla_m^2 [C42] - k_{42a}[C24m][C42] + k_{42d}[C42a] \quad (6)$$

$$\frac{\partial [C42a]}{\partial t} = D_m \nabla_m^2 [C42a] + k_{42a}[C24m][C42] - k_{42d}[C42a] \quad (7)$$

$$\frac{\partial [B1m]}{\partial t} = D_m \nabla_m^2 [B1m] + k_{B1cm}[C42a][B1c] - k_{B1mc}[B1m] \quad (8)$$

$$B1^* = \frac{B1_t^*}{1 + (\gamma[B1m])^{-h}}, \quad (9)$$

where $B1_t^* = \int_S [B1m]ds/SA$; $\gamma = SA/\left(2\int_S [B1m]ds\right)$. $SA = \int_S ds$, is the surface area of the cell.

$$Gbg_n^* = \frac{R}{1 + (\delta(Gbg_n))^{-q}}, \quad (10)$$

where $\delta = SA\int_S (Gbg_n)ds$, and $R = 1$ unless otherwise specified.

The initial conditions and conservation equations are as follows. We may assume that [C42], [R], and [G] are equally distributed along the surface with a total amount of $C42_t$, R_t and G_t, respectively.

$$[R]_0 = R_t/SA, R_t = 10,000 \text{ molecules/cell},$$
$$[G]_0 = G_t/SA, G_t = 10,000 \text{ molecules/cell},$$
$$[C42]_0 = C42_t/SA, C42_t = 10,000 \text{ molecules/cell},$$
$$[RL]_0 = 0, [Ga]_0 = 0, [C24m]_0 = 0, [C42a]_0 = 0, [B1m]_0 = 0.$$
$$[Gd] = [G]_0 - [G] - [Ga],$$
$$[Gbg] = [G]_0 - [G],$$
$$Gbg_n = [Gbg]/G_0,$$
$$V \cdot [C24c] = C24_t - \int_S [c24m]ds, C24_t = 2000 \text{ molecules/cell},$$
$$V \cdot [B1c] = B1_t - \int_S [B1m]ds, B1_t = 3000 \text{ molecules/cell}, V \text{ is the}$$
volume of the cell.

The cell was simulated as an axisymmetric ellipsoid possessing radii of $2\ \mu m$ (major axis) and $1\ \mu m$ (minor axis). The surface area and volume of the cell were $SA = 21.5\ \mu m^2$ and $V = 8.4\ \mu m^3$, respectively. The ligand gradient was administered along the major axis of the ellipsoid (i.e. axis of symmetry).

The rate constants are listed below:

$k_{RL} = 2 \times 10^6\ M^{-1}\ s^{-1}$; $k_{RLm} = 1 \times 10^{-2}\ s^{-1}$; $k_{Rs} = 4$ (molecules) s^{-1}/SA; $k_{Rdo} = 4 \times 10^{-4}\ s^{-1}$; $k_{Rd1} = 4 \times 10^{-4}\ s^{-1}$; $k_{G1} = 1$ (molecules)$^{-1}\ s^{-1} \times SA$; $k_{Ga} = 1 \times 10^{-5}$ (molecules)$^{-1}\ s^{-1} \times SA$; $k_{Gd} = 0.1\ s^{-1}$; $k_{24cm0} = 0.04\ s^{-1} \times V/SA$; $k_{24cm1} = 3.3 \times 10^{-3}$ (molecules)$^{-1}\ s^{-1} \times V$; $k_{24mc} = 1\ s^{-1}$; $k_{42a} = 1 \times 10^{-5}$ (molecules)$^{-1}\ s^{-1} \times SA$; $k_{42d} = 0.02\ s^{-1}$; $k_{B1cm} = 1 \times 10^{-5}$ (molecules)$^{-1}\ s^{-1} \times V$; $k_{B1mc} = 0.01\ s^{-1}$.

We modeled the response of an **a**-cell to α-factor (Fig. 1A). In the heterotrimeric G-protein cycle, the peptide pheromone α-factor (L) binds alpha-factor receptor (R) to form the active receptor complex (RL). The RL species catalyzes the activation of the heterotrimeric G-protein (G) to form active α-subunit (Ga) and free G$\beta\gamma$ (Gbg). Ga is deactivated to form inactive α-subunit (Gd), which binds to G$\beta\gamma$ to reform the heterotrimer.

In the Cdc42p cycle, the membrane-bound form of Cdc24p (C24m) activates Cdc42p (C42) to its active form (C42a). In turn, C42a is capable of binding the scaffold protein Bem1p (B1) and recruiting it to the membrane (B1m). Cytoplasmic Cdc24p (C24) can be brought to the membrane either by free G$\beta\gamma$ or by Bem1p.

The key amplification mechanism that facilitates polarization is the positive feedback loop in which membrane-associated Bem1p (B1m) binds and activates Cdc24p (C24m) which catalyzes the formation of active Cdc42p (C42a) which binds more Bem1p (Fig. 1A). Bem1p is a scaffold protein that is at the center of a protein-protein interaction network. [11] We modeled these multivalent binding

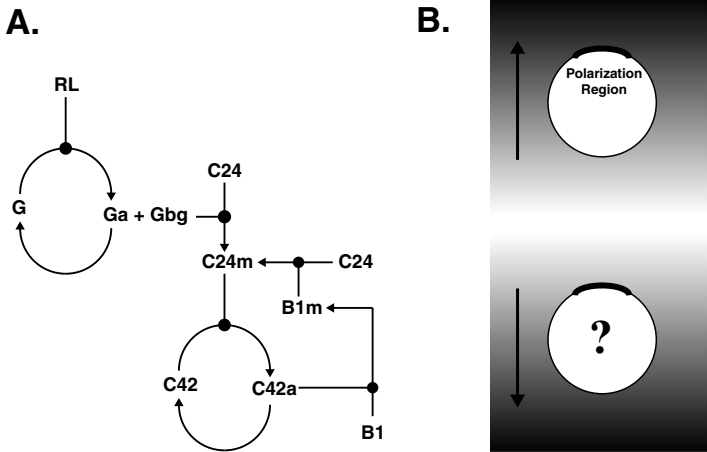**Modeling Yeast Cell Polarization Induced by Pheromone Gradients**

Fig. 1. Overview of yeast pheromone response system. (A) Schematic diagram of signal transduction pathway. The arrows indicate the conversion of one species into another. The solid dot represents a reaction catalyzed by the connected species. See text for details on species. (B) Amplification and tracking during yeast polarization. The top panel shows a yeast cell amplifying the external ligand gradient to produce an all-or-none polarization of a component at the front of the cell. The bottom panel asks what happens when the gradient is reversed. Is the cell able to repolarize in response to the change in gradient direction?

interactions using a Hill-type formula possessing a cooperativity parameter h. Thus, the amplifier depends on both positive feedback and cooperativity.

Our model incorporated lateral surface diffusion on the membrane. All the proteins were assumed to have the same surface diffusion coefficient D_m. We did not represent diffusion in the cytoplasm.

We assumed that the cell has an axisymmetric shape with the direction for the gradient of L as the axis of symmetry. The membrane of the cell then was represented in terms of two variables $(r(\alpha), z(\alpha))$ where α is a parametrization variable in $[0, \pi]$. The gradient of L on the cell membrane was assumed to be

$$L(r(\alpha), z(\alpha)) = L_{\text{ini}} + L_d(z(\alpha) - z(0))$$

where L_{ini} is the concentration of ligand at the tip of cell, and L_d is the slope of gradient of L along the length of the cell (major axis). For the simulations described here, $L_{\text{ini}} = 8$ nM and $L_d = 1$ nM/μm.

We have attempted to occupy the middle ground between a well-validated mechanistic model and a phenomenological generic model. Our goal was to explore performance constraints of gradient-sensing using a model that was approximately based on the real biological system. The primary reason why we chose this approach was that no quantitative data exists on the polarization of specific

proteins during gradient-sensing in yeast. Only one paper[12] has been published documenting the response of yeast cells to a pheromone gradient, but Segall did not examine the localization of proteins during gradient-induced polarization. In the model, we represent the species Ste2p, Gpalp, G$\beta\gamma$ (Ste4p/Stel8p), Cdc42p, Cdc24p, and Bem1p. The deletion of any of these species in yeast cells prevents polarization, and the model was able to reproduce this polarization-defective phenotype of the deletion mutants.

3. METHODS FOR SIMULATING CELLULAR SPATIAL DYNAMICS

The surface diffusion of a quantity W on an axisymmetric surface has a simple expression,

$$\nabla_m^2 W = W_{ss} + \frac{r_s W_s}{r} \tag{11}$$

where $s = \sqrt{z^2(\alpha) + r^2(\alpha)}$ is the arclength of the cell membrane. Consequently, Eqs. (1–8) becomes one-dimensional in terms of the parametrization variable α, even though the cell is a 3D axisymmetric ellipsoid.

Numerical discretizations of the concentration of the various proteins, such as [R] and [C42], on the cell membrane were carried out in $\alpha \in [0, \pi]$. A second-order finite difference discretization was used for all spatial derivatives. The collocation point, $\alpha_i = ih + h/2$ with $i = 0, 1, \ldots, N - 1$ and $h = \pi/N$, was chosen to be away from 0 and π, to avoid evaluation of zero denominators for many quantities. At α_0 and α_{N-1}, the symmetry of the concentration quantities was exploited for the approximated derivatives. A fourth order Adams-Moulton predictor-corrector method was implemented for the temporal approximation.

The simulations were reproducible for different mesh sizes (from $N = 16$ to $N = 256$) and for different time steps (from $\Delta t = 5 \times 10^{-4}$ s to $\Delta t = 2.5 \times 10^{-6}$ s). In our simulations, we typically used mesh sizes of $N = 16$ or $N = 32$ and a time step of $\Delta t = 5 \times 10^{-4}$ s.

4. SENSITIVITY DEPENDS ON POSITIVE FEEDBACK AND COOPERATIVITY

One of the major challenges of gradient-sensing is to amplify a shallow external signal to produce a dramatic polarization of internal components. Indeed, during the yeast pheromone response, the polarization appears to be all-or-none with some proteins found only at the front of the cell (T.-M. Yi, data not shown). In our model, we have proposed a novel amplification mechanism in which the scaffold protein Bemlp plays a central role serving to create a positive feedback loop and to nucleate a network of protein-protein interactions. These effects are represented in the B1* term, which possesses a Hill equation form, in Eq. (9).

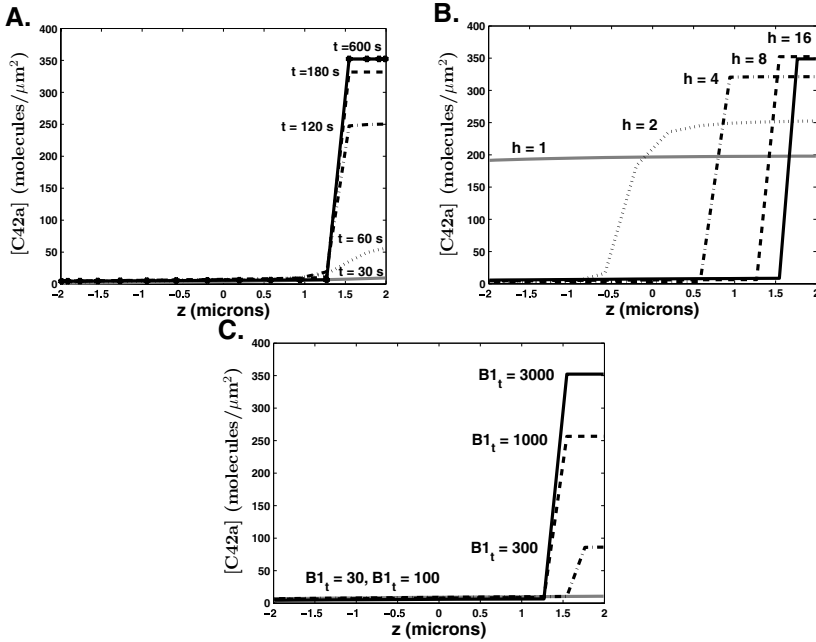**Modeling Yeast Cell Polarization Induced by Pheromone Gradients**

Fig. 2. Description of polarization. The x-axis denotes the position along the length of the cell. The y-axis denotes the concentration of active Cdc42p. (A) Time course of polarization. For $h = 8$, the polarization is shown from $t = 0$ to $t = 10$ min. (B) Cooperativity increases polarization. The polarization is shown for $h = 1, 2, 4, 8, 16$. (C) Dependence of polarization on levels of Bemlp. The variable B_t representing total Bemlp was varied from 30 (solid gray line) to 3000 (solid black line) molecules/cell with $h = 8$.

Simulations of this model displayed dramatic polarization of active Cdc42p (C42a). We turned off surface diffusion by setting $D_m = 0$. Polarization was observed within the first five minutes (Fig. 2A), which was a bit fast. In experiments, polarization is observed by 10 min (T.-M. Yi, data not shown). However, our model does not include dynamics such as the transport of Cdc24p from the nucleus to the cytoplasm that may introduce time delays.

Two key parameters are the Hill constants in Gbg_n^* (q) and B1* (h). The parameter q describes the cooperativity of the activation of Cdc24p by $G\beta\gamma$, but it is not involved in the positive feedback loop. We explored a range of values for q from 1 to 100, and settled on 10 to reflect a significant degree of cooperativity. Overall, polarization was not sensitive to q. On the other hand, amplification was quite sensitive to h. Increasing h from 1 to 16 caused the polarization of C42a to increase significantly (Fig. 2B).

We were also interested in the effect of weakening the positive feedback loop. This was accomplished by decreasing the total amount of Bemlp ($B1_t$), which reduced the numerator in the $B1^*$ term. Interestingly, there was a sharp dependence on levels of Bemlp (with $h = 8$). Below a threshold, no polarization was observed ($B1_t = 30$, $B1_t = 100$; Fig. 2C). Beyond the threshold, the amount of active Cdc42p at the front of the cell increased as $B1_t$ increased. One biological interpretation of this result is that at low levels of Bemlp, there would be no projection at all, and then at higher levels the projection would increase in size as more Bemlp was synthesized.

5. TRADEOFF BETWEEN AMPLIFICATION AND TRACKING

A good gradient sensor can track a change in the gradient direction. After applying the gradient in one direction and simulating the polarization response, we switched the gradient $180°$ to see if the polarization flipped sides. Interestingly, we found that the polarization remained fixed in the former forward direction for larger values of h (e.g. $h = 4$, Fig. 3). We interpreted this behavior to result from the bistable nature of the system. Bistability is known to be a property of positive feedback systems that possess open-loop input-output ultrasensitivity,[13] which can arise from cooperativity.
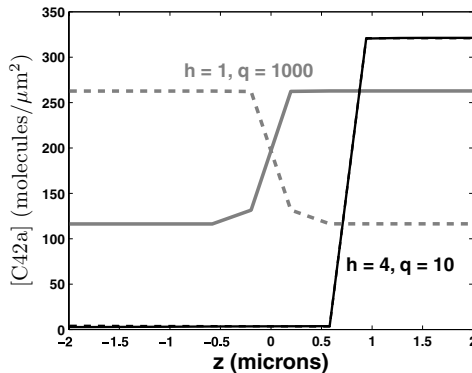

Fig. 3. Polarization and bistability. The gradient was initially set from right (high) to left (low), and then flipped $180°$. The solid lines represent the initial polarization and the dashed lines represent the polarization after the gradient direction had been switched. For larger values of h (e.g. $h = 4$), the polarization was pronounced (solid black line), but was unresponsive to a reversal in the gradient direction (dashed black line almost completely overlaps solid black line). Increasing the cooperativity of $G\beta\gamma$ activation of Cdc24p ($q = 1000$) while keeping $h = 1$ resulted in a modest level of amplification (solid gray line) that was able to track the change in gradient direction (dashed gray line).

There was an apparent tradeoff between the amplification and tracking. Small values of h (e.g. $h = 1$) produced little to no amplification, but were not bistable. Larger values of h produced more amplification, but also exhibited bistability.

In our model, amplification arises from the two terms Gbg_n^* and $B1^*$, with the main contribution from $B1^*$. Because Gbg does not belong to the positive feedback loop, its spatial dynamics do not get trapped by the bistable behavior. Thus, we hypothesized that increasing the cooperativity of Gbg_n^* would increase amplification without affecting tracking. Indeed, letting $q = 1000$ ($h = 1$, $R = 100$) resulted in a modest degree of polarization of active Cdc42p while still allowing the polarization to follow the reversal in gradient direction. Nevertheless, the extent of polarization was considerably smaller than when h was increased.

6. EFFECT OF SURFACE DIFFUSION AND REGULATION OF SURFACE DIFFUSION ON POLARIZATION

The membrane lipid bilayer is fluid, and proteins are able to diffuse in the plane of the membrane.[14,15] The two-dimensional diffusion coefficient for an integral membrane protein can range as high as $1 \ \mu m^2/s$ to as low as 0 (immobile). In our model, the two-dimensional surface diffusion coefficients for all the protein components were set to be equal to the same value, D_m. In the simulations described above, $D_m = 0$. We expected that the inclusion of surface diffusion would reduce the degree of polarization. To test this, we examined the polarization at values of the diffusion coefficient ranging from 0.001 to 0.1 $\mu m^2/s$.

Figure 4A shows a quantitative decline in polarization with increasing surface diffusion, and when $D_m = 0.1 \ \mu m^2/s$, polarization was almost completely eliminated. These simulations demonstrate the critical importance of including surface diffusion in the calculations. How then does polarization occur in cells if lateral diffusion is so potent at dissipating proteins localized to a particular region?

There is abundant evidence that the plasma membrane is quite heterogenous and that lateral diffusion can be restricted by the cytoskeleton.[16] In yeast, it is known that the septins can act as a diffusion boundary during the polarization that accompanies budding.[17] In our model, we proposed that $G\beta\gamma$ may influence the formation of a diffusion barrier. Thus, we assigned D_m to be the following:

$$D_m = \frac{D_{\max}}{1 + (\beta(Gbg_n))^n}, \tag{12}$$

where $\beta = SA / \int_s (Gbg_n)ds$. D_m is smaller in regions of the cell surface where there is more free $G\beta\gamma$.

One can think of n as a cooperativity parameter on how $G\beta\gamma$ influences diffusion. We explored values of n from $n = 10$ to $n = 1000$. As we increased n, D_m approached 0 at the front of the cell, and the polarized proteins did not diffuse
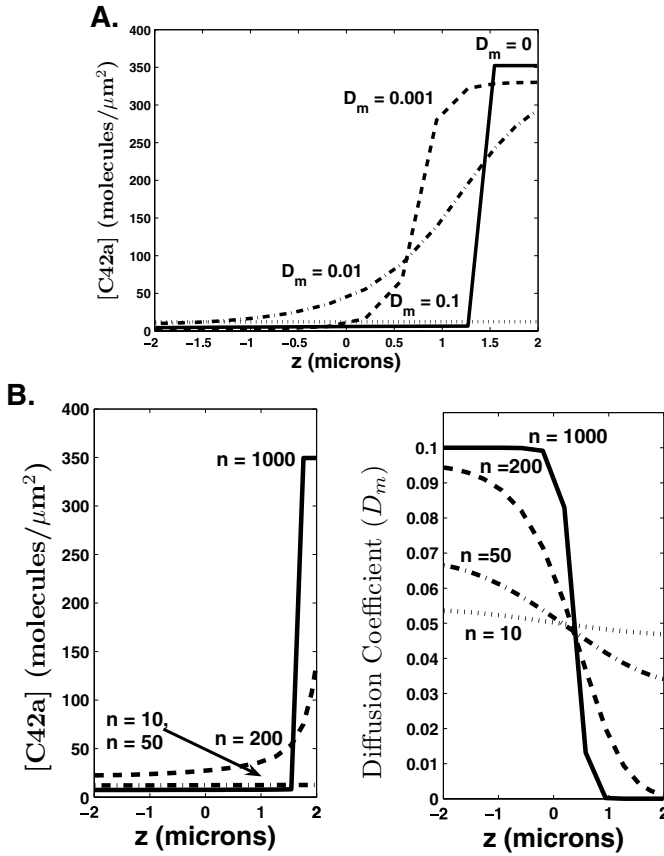
Fig. 4. Effect of surface diffusion on polarization. (A) Increasing lateral diffusion decreases polarization. With $h = 8$, we plotted the polarization of C42a at 10 min for different values of the diffusion coefficient D_m. (B) Regulation of lateral diffusion by G$\beta\gamma$, Eq. (12), restores polarization. For small n, there was no polarization (left panel), and D_m was only slightly smaller in the front versus the back (right panel). For large n, there was polarization, and D_m approached 0 at the front of the cell.

away as much. Only at $n = 200$, however, did we observe signs of polarization. When $n = 1000$, full polarization was once again achieved (Fig. 4B). Full polarization was only achieved with large n because the spatial variation of (Gbg_n) was small, and therefore the quantity $\beta(Gbg_n)$ was close to 1. In our simulations, the value of $\beta(Gbg_n)$ ranged approximately from 0.98 to 1.02. These simulations indicated that the regulation of lateral diffusion has to be quite significant to restore polarization in our model. In yeast, the septins do have an all-or-none localization at the front of the cell during the pheromone response,[18] and if they are acting as a diffusion barrier, then large values of n may be biologically plausible.
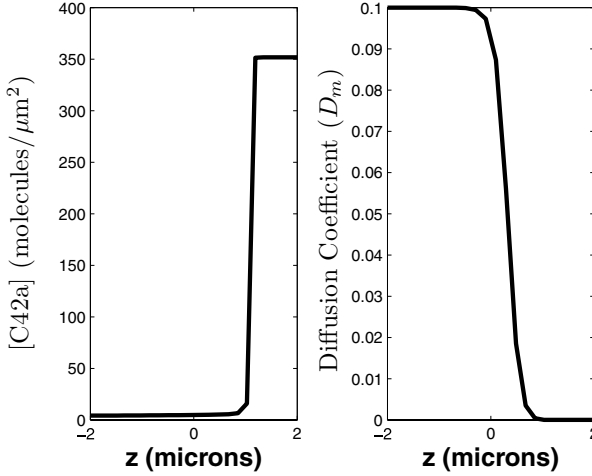
Fig. 5. Polarization using alternative regulated lateral diffusion expression (Eq. (13)). With $h = 8$, $q = 10$, $\tau = 20$ and $m = 50$, we plotted the polarization of C42a at 200 sec (left panel) and the regulated diffusion coefficient D_m (right panel). Significant polarization was observed for less extreme values of the modified cooperativity parameter m.

We explored another possible formula for regulated lateral diffusion that did not require such large cooperativity parameter values:

$$D_m = \frac{D_{max}}{1 + [1 + \tau(\beta(Gbg_n) - 1)]^m},\tag{13}$$

where τ is a constant and β is defined as in Eq. (12). One can view this expression as a modified form of the Hill equation which incorporates additional interactions into the Gbg_n term. The key was that polarization was restored using a smaller value of m, the new cooperativity parameter. Indeed, a value of $m = 50$ resulted in substantial polarization (Fig. 5).

We then tested whether the model using the regulated diffusion described in Eq. (12) with $n = 1000$ would allow tracking. Interestingly, after reversing the gradient, active Cdc42p repolarized on the opposite side but the new polarization was different from the original polarization indicating the existence of a second steady-state (Fig. 6B). Multiple steady-states were observed for large values of h and n including some in which there was no polarization when the gradient was reversed (i.e. unpolarized stable steady-state).

7. ACHIEVING BOTH AMPLIFICATION AND TRACKING

We hypothesized that combining the mechanisms from the previous two sections (regulated surface diffusion and cooperative activation of Cdc24p by G$\beta\gamma$)
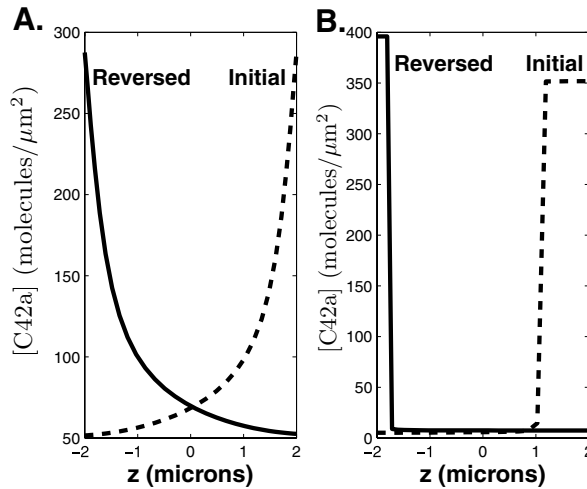
Fig. 6. Tracking directional changes in the gradient. (A) In this model, $h = 8$, $q = 100$, and $n = 200$. The initial gradient was applied for 20 minutes and then the direction was reversed for another 20 minutes. The polarization of C42a is shown for $t = 20$ min (dashed line) and $t = 40$ min (solid line). (B) Multiple steady-states for high values of h and n. For this simulation, $h = 8$, $q = 10$, and $n = 1000$. Reversing the initial gradient resulted in repolarization that was different from the original polarization, indicating the existence of a second steady-state.

could improve the ability of the cell to both amplify and track a gradient signal. The intuition is that splitting the amplification between the two G-protein cycles may prevent the bistability that arises from the overly potent positive feedback produced by the Cdc42p cycle dynamics when the Bem1p cooperativity parameter h is large. By setting $q = 100$, $n = 200$, and $h = 8$ we could indeed obtain polarization that was able to follow $180°$ changes in the gradient direction (Fig. 6A). Achieving high amplification that can track the gradient reversal proved to be a challenging task in our model, and it is interesting that we needed to take into account lateral diffusion to make it work.

The change was relatively slow, and it required fine-tuning of the parameters. For example, decreasing D_{max}, increasing h, or increasing n would cause the cell to become stuck in an unpolarized state after flipping the gradient or to go to a new polarized steady-state (Fig. 6B). On the other hand, increasing D_{max}, decreasing h, or decreasing n would reduce the initial polarization.

This type of fragility suggests that additional control mechanisms must be in place to make this system more robust. In particular, we believe that including the regulated dynamics for the production and degradation of the system components would ensure more reliable amplification and tracking of gradients by the model.

8. CONCLUSION

Here we proposed a novel mechanism and model for producing sensitivity and tracking of pheromone gradients by yeast. The amplification depended on a positive feedback loop involving the scaffold protein Bem1p and cooperative binding. The regulation of surface diffusion of proteins on the membrane and balancing the amplification between the two G-protein cycles contributed to tracking.

We believe that the unrealistically large values for certain Hill coefficients (e.g. q and n) indicate the presence of unmodeled dynamics that are not captured by the current model. In this context, the Hill equation is serving as a descriptive proxy for the true reaction kinetics that give rise to the system behavior. Future improved versions of the model will replace these Hill equations with more detailed mechanistic equations that may involve additional positive feedback loops, cascades of cooperative protein-protein interactions, or other amplification mechanisms.

In the chemotaxis literature, one popular class of models invokes a "local excitation, global inhibition" mechanism to promote directional-sensing;[19] there is a balance between rapid local activation and slower global inhibition. Our model falls into the category of a "positive feedback" model with the emphasis on powerful internal positive feedback loops. One can argue, however, that there is indirect global inhibition represented in the normalization of the $B1^*$ and Gbg_n^* terms. In addition, our model is different because it focuses on the spatial dynamics at the cell surface, especially the localized recruitment of proteins to a point taking advantage of positive feedback and cooperative binding. Factors such as surface diffusion and dissociation from the membrane into the cytoplasm act to limit the polarization.

One goal of Systems Biology is to help make sense of the complexity of living systems. Qualitative arrow diagrams are ill-suited for explaining dynamical processes such as gradient-sensing. Previous mathematical models of the yeast pheromone response system did not explicitly represent spatial dynamics. We hope that this research serves as a first step toward elucidating the relationship between complex biological networks such as signal transduction pathways and complex behaviors such as polarization and mating in yeast.

There are numerous areas in which our models can be improved. In particular, many important reactions and components were missing. These included a treatment of gene regulation by pheromone via the MAPK (Mitogen-Activated Protein Kinase) pathway, the synthesis and degradation of the various G-protein components, the transport of Cdc24p from the nucleus to the cytoplasm, and the dynamics and regulation associated with the actin cytoskeleton. In addition, we did not model many of the negative feedback loops, and there was no consideration of external and internal noise. These issues will be addressed in the future.

There are several notable predictions and outcomes derived from this work. First, we argued that both G-protein cycles must contribute to the amplification in order to achieve polarization that can follow directional changes. Second, our modeling suggested that there will be a quantitative dependence of polarization on the levels of the scaffold protein Bem1p. Third, we explained why the regulation of diffusion may be useful for robust gradient-sensing. Finally, it is evident that novel mechanisms must exist, not explored here, so that yeast cells possess the capability of detecting rapid and subtle changes in the direction of the pheromone gradient in a robust fashion.

ACKNOWLEDGMENT

REFERENCES

1. D. G. Drubin and W. J. Nelson, Origins of cell polarity. *Cell* **84**:335–344 (1996).
2. A. G. Gilman, *et al.*, Overview of the alliance for cellular signaling. *Nature* **420**:703–706 (2002).
3. G. F. Sprague Jr. and J. W. Thorner, in *The Molecular and Cellular Biology of the Yeast Saccharomyces: Gene Expression* (Cold Spring Harbor Laboratory Press, Cold Spring Harbor, 1992).
4. H. G. Dohlman and J. W. Thorner, Regulation of G protein-initiated signal transduction in yeast: Paradigms and principles. *Annu. Rev. Biochem.* **70**:703–754 (2001).
5. D. Pruyne and A. Bretscher, Polarization of cell growth in yeast: I. Establishment and maintenance of polarity states. *J. Cell Sci.* **113**:365–375 (2000).
6. C. L. Jackson, J. B. Konopka and L. H. Hartwell, *S. cerevisiae* alpha pheromone receptors activate a novel signal transduction pathway for mating partner discrimination. *Cell* **67**:389–402 (1991).
7. N. Hao, N. Yildirim, Y. Wang, T. C. Elson and H. G. Dohlman, Regulators of G protein signaling and transient activation of signaling: Experimental and computational analysis reveals negative and positive feedback controls on G protein activity. *J. Biol. Chem.* **278**:46506–46515 (2003).
8. B. Kofahl and E. Klipp, Modelling the dynamics of the yeast pheromone pathway. *Yeast* **21**:831–850 (2004).
9. T.-M. Yi, H. Kitano and M. I. Simon, A quantitative characterization of the yeast heterotrimeric G protein cycle. *Proc. Natl. Acad. Sci. USA* **100**:10764–10769 (2003).
10. S. Sivakumaran, S. Hariharaputran, J. Mishra and U. S. Bhalla, The database of quantitative cellular signaling: Management and analysis of chemical kinetic models of signaling networks. *Bioinformatics* **19**:408–415 (2003).
11. A. C. Butty, N. Perrinjaquet, A. Petit, M. Jaquenoud, J. E. Segall, K. Hofmann, C. Swahlen and M. Peter, A positive feedback loop stabilizes the guanine-nucleotide exchange factor Cdc24 at sites of polarization. *EMBO J.* **21**:1565–1576 (2002).
12. J. E. Segall, Polarization of yeast cells in spatial gradients of alpha mating factor. *Proc. Natl. Acad. Sci. USA* **90**:8332–8336 (1993).
13. D. Angeli, J. E. Ferrell, Jr. and E. D. Sontag, Detection of multistability, bifurcations, and hysteresis in a large class of biological positive-feedback systems. *Proc. Natl. Acad. Sci. USA* **101**:1822–1827 (2004).

14. K. Jacobson, A. Ishihara and R. Inman, Lateral diffusion of proteins in membranes. *Annu. Rev. Physiol.* **49**:163–175 (1987).
15. K. Suzuki, K. Ritchie, E. Kajikawa, T. Fujiwara and A. Kusumi, Rapid hop diffusion of a G-protein-coupled receptor in the plasma membrane as revealed by single-molecule techniques. *Biophys. J.* **88**:3659–3680 (2005).
16. F. R. Maxfield, Plasma membrane microdomains. *Curr. Opin. Cell Biol.* **14**:483–487 (2002).
17. J. Dobbelaere and Y. Barral, Spatial coordination of cytokinetic events by compartmentalization of the cell cortex. *Science* **305**:393–396 (2004).
18. A. Nern and R. A. Arkowitz, G proteins mediate changes in cell shape by stabilizing the axis of polarity. *Mol. Cell* **5**:853–864 (2000).
19. P. Devreotes and C. Janetopoulos, Eukaryotic chemotaxis: Distinctions between directional sensing and polarization. *J. Biol. Chem.* **278**:20445–20448 (2003).